



**HAL**  
open science

## Miniaturized notch antenna based on lanthanum titanium perovskite oxide thin films

Hoai-Nam Nguyen, Ratiba Benzerga, Christophe Delaveaud, Claire Le Paven-Thivet, Yu Lu, Ala Sharaiha, Laurent Le Gendre, Stéphanie Députier, Franck Tessier, François Cheviré, et al.

► **To cite this version:**

Hoai-Nam Nguyen, Ratiba Benzerga, Christophe Delaveaud, Claire Le Paven-Thivet, Yu Lu, et al.. Miniaturized notch antenna based on lanthanum titanium perovskite oxide thin films. *Thin Solid Films*, 2014, 563, pp.36-39. 10.1016/j.tsf.2014.04.011 . hal-01023630

**HAL Id: hal-01023630**

**<https://hal.science/hal-01023630v1>**

Submitted on 16 Sep 2024

**HAL** is a multi-disciplinary open access archive for the deposit and dissemination of scientific research documents, whether they are published or not. The documents may come from teaching and research institutions in France or abroad, or from public or private research centers.

L'archive ouverte pluridisciplinaire **HAL**, est destinée au dépôt et à la diffusion de documents scientifiques de niveau recherche, publiés ou non, émanant des établissements d'enseignement et de recherche français ou étrangers, des laboratoires publics ou privés.

# Miniaturized notch antenna based on lanthanum titanium perovskite oxide thin films

H. Nguyen<sup>a b</sup>, R. Benzerga<sup>a</sup>, C. Delaveaud<sup>b</sup>, C. Le Paven<sup>a</sup>, Y. Lu<sup>a</sup>, A. Sharaiha<sup>a</sup>, L. Le Gendre<sup>a</sup>, S. Députier<sup>c</sup>, F. Tessier<sup>c</sup>, F. Cheviré<sup>c</sup>, X. Castel<sup>a</sup>

a. Institut d'Electronique et de Télécommunications de Rennes (IETR, UMR-CNRS 6164), IUT Saint Briec, Université de Rennes 1, 22004 Saint Briec, France

b. CEA-LETI Minatec Campus, 17 Rue des Martyrs, 38054 Grenoble, France

c. Institut des Sciences Chimiques de Rennes (ISCR, UMR-CNRS 6226), Université de Rennes 1, 35000 Rennes, France

## Abstract

This paper presents the integration of a dielectric lanthanum titanium oxide compound as thin film in a discrete capacitive component operating at microwaves. The integration in a notch antenna of a MIM (Metal/Insulator/Metal) structure based on this oxide material is numerically and experimentally studied. Oxide films are deposited by reactive magnetron RF sputtering of an  $\text{La}_2\text{Ti}_2\text{O}_7$  target. The films are composed of an unusual phase: the orthorhombic  $\text{La}_2\text{Ti}_2\text{O}_7$  compound, with a textured growth on Pt/Si and Pt/SrTiO<sub>3</sub> substrates. Moderate dielectric constant values (Epsilon around 60) and low loss (Tan Delta lower than 0.005) are obtained at 1 GHz. Inserting this original MIM capacitor in the antenna structure results in a shift to a lower value of its operating frequency. This shift, from 885 MHz to 317 MHz, corresponds to a significant size reduction of 64.2%. The measured values are confronted with simulation obtained by numerical software.

## Keywords

Thin films ; Titanate ; Miniaturization ;  $\text{La}_2\text{Ti}_2\text{O}_7$  ; Microwaves ; Sputtering deposition ; Antenna ; Dielectric

## 1. Introduction

The generalization of wireless communicating objects has intensified the need for miniaturization of integrated devices, in particular antennas. Many techniques have been developed [1], including the use of localized capacitive loading based on a dielectric thin film [2], [3] that can be used in different antenna topologies. Z. Ma et al. [4] reported on a capacitor composed of two concentric electrodes deposited on  $\text{Ba}_{1-x}\text{Sr}_x\text{TiO}_3$  (BST)/Pt substrate, the perovskite BST compound being the dielectric material. However, this configuration suffered from very high capacitance and dielectric loss values [5], not consistent with those required for antenna miniaturization.

In the present paper, we introduce a capacitor based on perovskite-type oxide  $\text{La}_2\text{Ti}_2\text{O}_7$  (LTO) dielectric thin films and detail their integration in a slot antenna. Our previous studies on thin film deposition [6], [7] and dielectric characterization [8] of  $\text{La}_2\text{Ti}_2\text{O}_7$  oxide and  $\text{LaTiO}_2\text{N}$  oxynitride compounds have shown that the oxide films present loss less than 0.02 at 10 GHz. In the present work, particular design is carried out to integrate the LTO based MIM (Metal/Insulator/Metal) components in a slot antenna structure. Special attention is given to the miniaturization ratio and to the loss introduced by the LTO based-component.

## 2. Calculation

The MIM structure is made of two concentric metallic disks (radii  $R$  and  $r$ ) deposited on the dielectric LTO layer (Fig. 1), that is itself deposited on conductive substrates, such as platinized substrates (silicon or  $\text{SrTiO}_3$ ). The value of the total capacitance corresponds to the capacitance formed by the central disk [4], and is controlled by the film thickness and dielectric constant, and the central disk diameter.

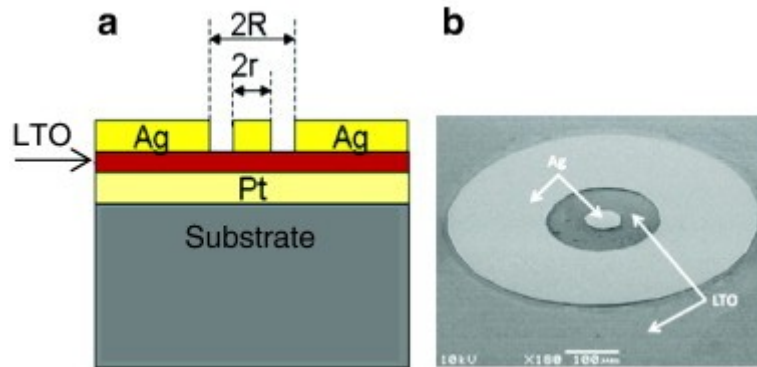


Fig. 1. MIM capacitor structure based on  $\text{La}_2\text{Ti}_2\text{O}_7$  (LTO) dielectric oxide films. (a) Schematic cross-section view and (b) scanning electron microscopy image.

The antenna structure consists of a notch cut from the edge of the ground plane. It is the complementary structure of a conventional quarter wavelength monopole antenna. This structure shows easy integration in printed circuit and significant miniaturization ratio when loaded with a correctly positioned capacitor [9]. The antenna is loaded with the MIM structure at the open end of the slot (Fig. 2). The slot length is  $L = 44.6 \text{ mm}$  ( $\sim \lambda_0/47$ ;  $F_0 = 900 \text{ MHz}$ , without capacity) and its width is  $W = 2 \text{ mm}$ . The antenna is fed by coupling with a microstrip line and the impedance matching is achieved by varying the position of the supply line ( $a$ ) and the stub length ( $L_f$ ). The substrate used here is FR4 polymer, with a thickness of  $0.8 \text{ mm}$ , a dielectric constant  $\epsilon_r \sim 4.4$  and a loss tangent of  $0.02$  at  $1 \text{ GHz}$ . The microstrip line has a width of  $1.51 \text{ mm}$  to obtain a  $50 \Omega$  characteristic impedance.

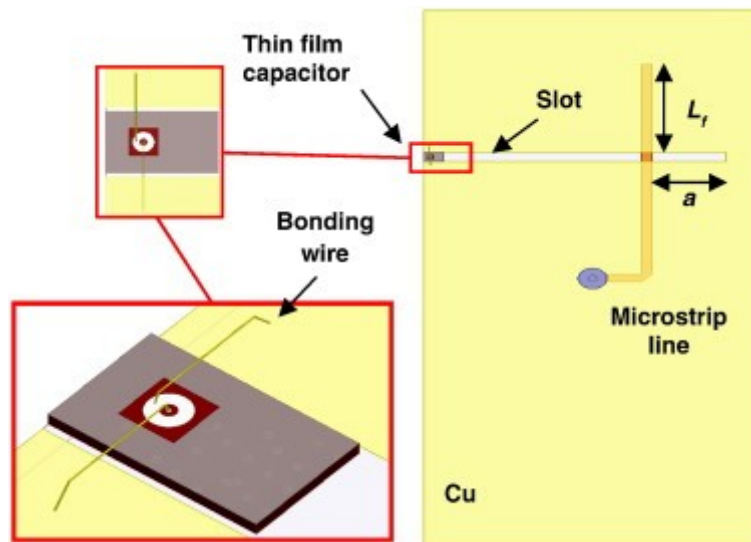


Fig. 2. Loaded antenna design based on localized MIM capacitor.

The simulation of this configuration was performed with Ansoft HFSS v13 [10], using  $R = 80 \mu\text{m}$ . Fig. 3a presents the evolution in function of the frequency of the reflection coefficient  $S_{11}$ , for various central disk radius  $r$  values, that is different capacitance values. For these simulations, a dielectric constant of  $60$  [8] and a thickness of  $500 \text{ nm}$  were used for the dielectric LTO thin film; different  $r$  radius values from  $20$  to  $40 \mu\text{m}$  were used. We observe a shift of the antenna reflection coefficient towards low frequencies as the disk radius

increases. As a result, the loaded antenna can work at a lower frequency than that imposed by its dimension, which corresponds to a miniaturization of the antenna. Simultaneously, as expected [9] and as shown in Fig. 3b, the antenna radiating efficiency drops rapidly from 62% to 12%. Consequently, a trade-off between miniaturization ratio and antenna efficiency should be considered.

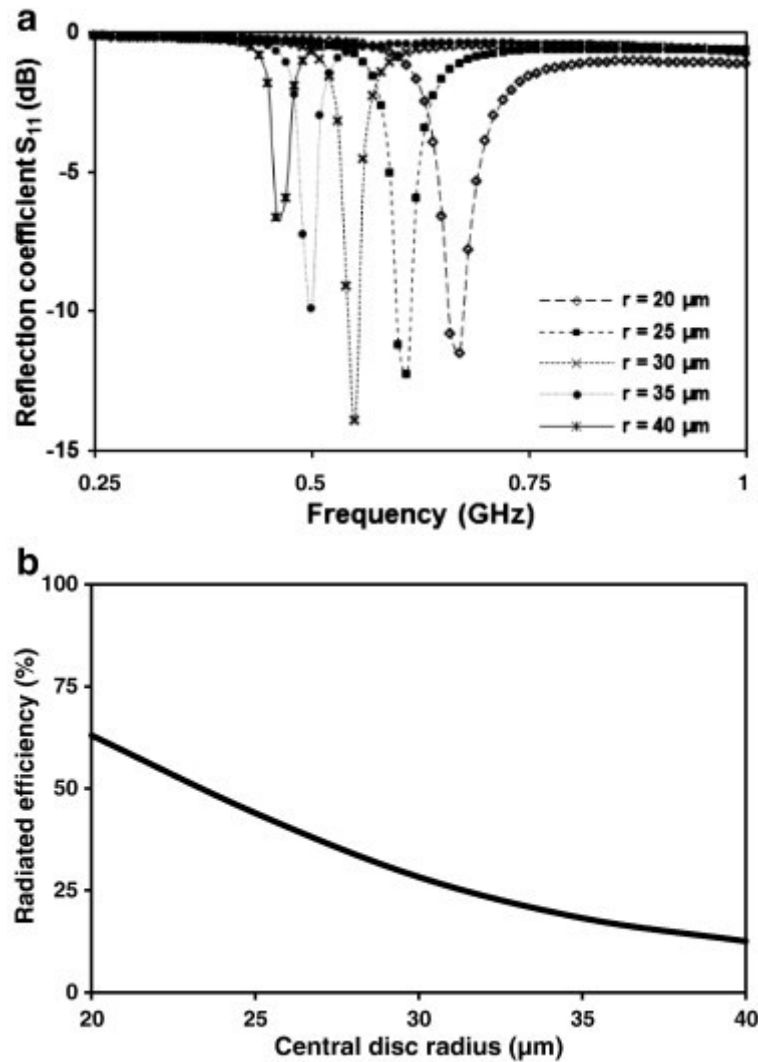


Fig. 3. (a) Simulated reflection coefficient as a function of frequency for different central disk radius  $r$  values and (b) simulated radiated efficiency as a function of central disk radius, of antennas based on  $\text{La}_2\text{Ti}_2\text{O}_7$  dielectric oxide films.

### 3. Experimental details

#### 3.1. Dielectric LTO thin film deposition

The LTO thin films are deposited by RF magnetron sputtering (Plassys MP4505S) on conducting substrates (Pt/Si and Pt/SrTiO<sub>3</sub> substrates) from a homemade  $\text{La}_2\text{Ti}_2\text{O}_7$  oxide target. For these depositions, the RF power ( $P_{\text{RF}}$ ) is fixed at  $1.8 \text{ W}\cdot\text{cm}^{-2}$ , the substrate temperature ( $T_s$ ) is  $800 \text{ }^\circ\text{C}$  and a total pressure ( $P_T$ ) of  $3.6 \text{ Pa}$  is used. The oxygen concentration in the process gas mixture, defined as  $[\text{O}_2/(\text{Ar} + \text{O}_2)]$ , is 25 vol.%. For this study, two different thicknesses of films (470 nm for LTO-1/Pt/Ti/SiO<sub>2</sub>/Si sample and 1200 nm for LTO-2/Pt/SrTiO<sub>3</sub> sample) are tested. The LTO films are identified by X-ray diffraction as the  $\text{La}_2\text{Ti}_2\text{O}_7$  compound with an orthorhombic crystalline cell [11]; they are (011) textured on platinized substrates.

### 3.2. MIM capacitor design and implementation

Concentric metallic disks constituting the upper electrodes of the MIM structure are made by standard photolithography and wet-etching of a metallic bilayer. This metallization is realized by magnetron sputtering deposition; the used parameters are:  $P_{RF} = 150$  W,  $T_S = T_{Amb}$  ( $\sim 20$  °C) and  $P_T = 1$  Pa. The bilayer is formed of a 2  $\mu\text{m}$ -thick silver film and a 5 nm-thick titanium film, the latter being used to ensure the adherence between the metallic layer and the LTO oxide film. Silver is chosen because of its high electric conductivity ( $\sigma \sim 6.1 \cdot 10^7$  S/m). The platinum layer of the substrate serves as the lower floating electrode of the MIM structure.

The notch antenna is printed on a standard FR4 substrate chosen for its low cost. The MIM capacitor is placed at the open end of the notch. The connections between concentric electrodes and the ground plane are made by a 25 micron diameter of gold bonding-wires (Fig. 4a).

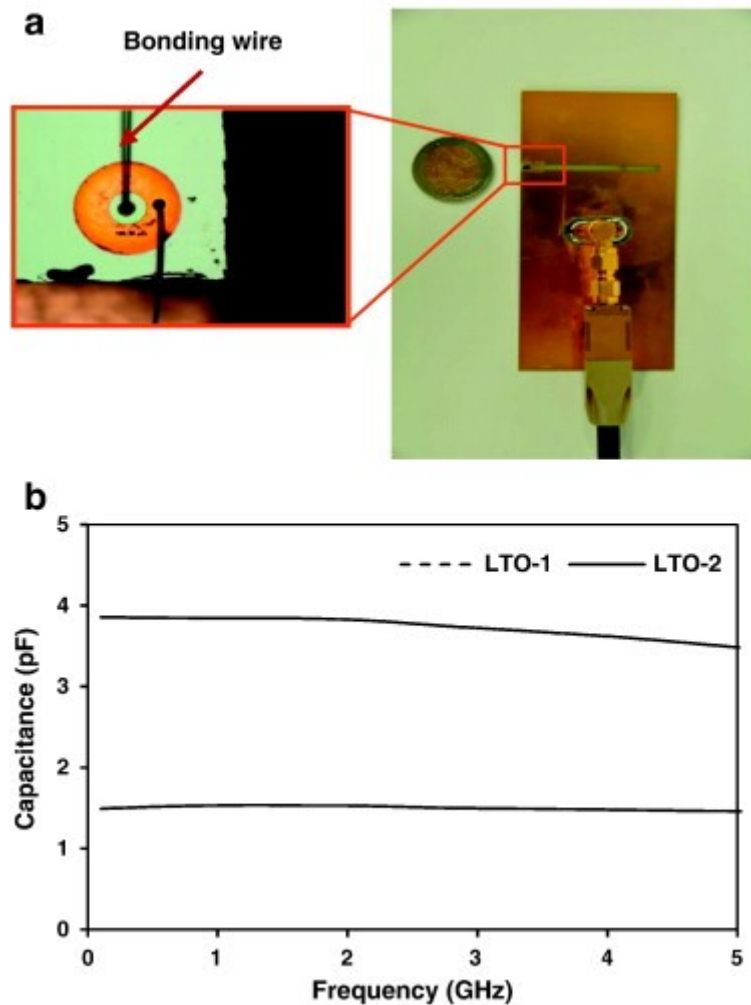


Fig. 4. (a) Antenna prototype based on a  $\text{La}_2\text{Ti}_2\text{O}_7$ -MIM structures and (b) variation of the capacitance of MIM structure based on LTO-1 and LTO-2 thin film samples, as a function of the frequency.

### 3.4. RF characterization

The characterization of the MIM capacitor is achieved by using a network analyzer (Agilent 8510C) associated with a microprobe station (Signatone H100). The Ground-Signal-Ground probes, which have a pitch of 150  $\mu\text{m}$ , are provided by Picoprobe. The intrinsic parameters (dielectric constant  $\epsilon'$  and loss  $\tan\delta$ ) of  $\text{La}_2\text{Ti}_2\text{O}_7$  thin films are obtained from the measurement of the  $S_{11}$  reflection coefficient of the MIM capacitor and from a RF differential extraction method developed in [4]. The radiation measurement of antenna prototypes is carried out in a large anechoic chamber.

## 4. Results and discussion

Concerning the intrinsic properties of  $\text{La}_2\text{Ti}_2\text{O}_7$  films, measurements of MIM structures (Fig. 4b) give capacitance values of 1.5 and 3.8 pF at 1 GHz for LTO-1 and LTO-2 samples respectively. The experimental central disk radii are 33 and 32  $\mu\text{m}$ ; the dielectric constant values are 64 and 61, with loss tangent values of 0.004 and 0.003 at 1 GHz for, respectively, LTO-1 and LTO-2.

The evolution in function of the frequency of the measured and simulated reflection coefficients  $S_{11}$  of the antennas based on LTO-1 and LTO-2 films is shown in Fig. 5. We note that the operating frequency shifts to lower values after the integration of MIM capacitors. The antenna with LTO-1, originally operating at 885 MHz, is shifted by 252 MHz to operate at 633 MHz, which corresponds to a miniaturization rate of 28.5%. For the antenna with LTO-2, the displacement in frequency from 568 MHz to 317 MHz induces a miniaturization rate of 64.2%. These miniaturization rates are summarized in Table 1 and are calculated by the following formula (1):

$$MR(\%) = \left| \frac{F_{loaded} - F_0}{F_0} \right| \times 100 \quad (1)$$

where  $F_{loaded}$  is the adaptation frequency of loaded antenna and  $F_0$  is the adaptation frequency of unloaded antenna.

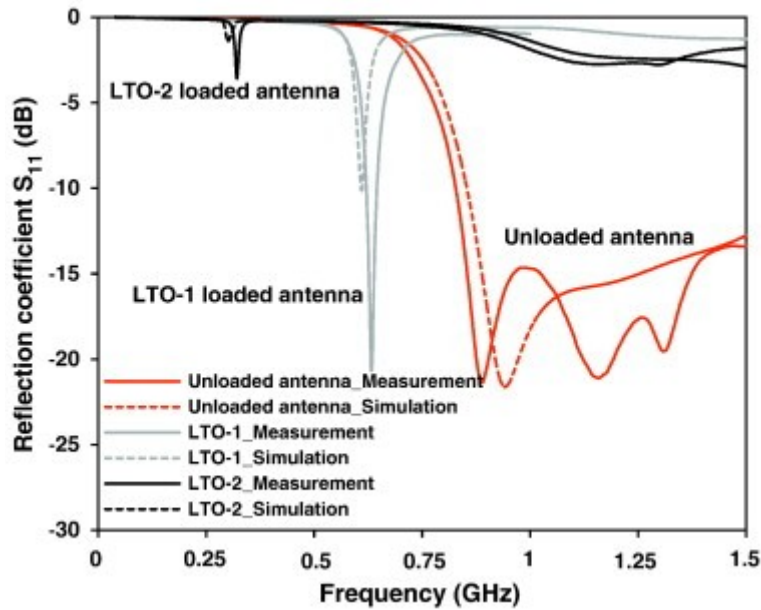


Fig. 5. Measurements (dashed line) and simulations (solid line) of the reflection coefficient  $S_{11}$  of antennas based on  $\text{La}_2\text{Ti}_2\text{O}_7$  dielectric oxide films.

Table 1. Simulated and measured performances of antenna prototypes based on  $\text{La}_2\text{Ti}_2\text{O}_7$  (LTO) dielectric oxide films.

Antenna prototypes	Capacitance (pF)	Adaptation frequency		Miniaturization rate	
		$F_a$ (MHz)		MR (%)	
		Measurement	Simulation	Measurement	Simulation
Without capacitor	0	885	940	0	0
With LTO-1	1.5	633	620	28.5	34
With LTO-2	3.8	317	300	64.2	68

A degradation of the bandwidth after the integration of LTO films is observed, in addition to a lack of antenna's impedance matching. This is due to an antenna impedance locus change with the significant frequency downshift. However, this antenna keeps a dipole radiation pattern for which omnidirectional

properties are preserved. Finally, Fig. 5 underlines the consistency of the experimental results with those of simulation.

Fig. 6 shows the total efficiency of the antenna with the LTO-1 MIM capacitor in comparison with a 1.8 pF commercial low loss SMD (Surface Mounted Device) capacitor. The measured efficiency is obtained by the integration of the gain pattern of the antenna in 3 dimensions. The antenna with the LTO-1 capacitor is matched for 630 MHz, whereas the one with SMD capacitor is matched for 590 MHz. The antenna using SMD capacitor reaches a higher efficiency (37%) than with the LTO-1 capacitor (30%); it also shows a good agreement between measurement and simulation. This agreement is not found for the LTO-1 based antenna, with a simulated efficiency of 50% and an experimental value of 30%. This deviation can be due, not to a lower quality of the LTO capacitance, but to the modeling approximations used in the simulation for the properties of the dielectric material, the thickness of conductors and for the antenna implementation (effect of the bonding connection, length and contact quality). Moreover, the thickness of the metallization (2  $\mu\text{m}$ ) was optimized for a working frequency up to 1 GHz, while the actual prototype radiates around 600 MHz. The loss skin effect at this frequency is quite substantial and can also be the cause of the difference observed between simulation and measurement. A higher thickness of metallization would be necessary to overcome this skin effect.

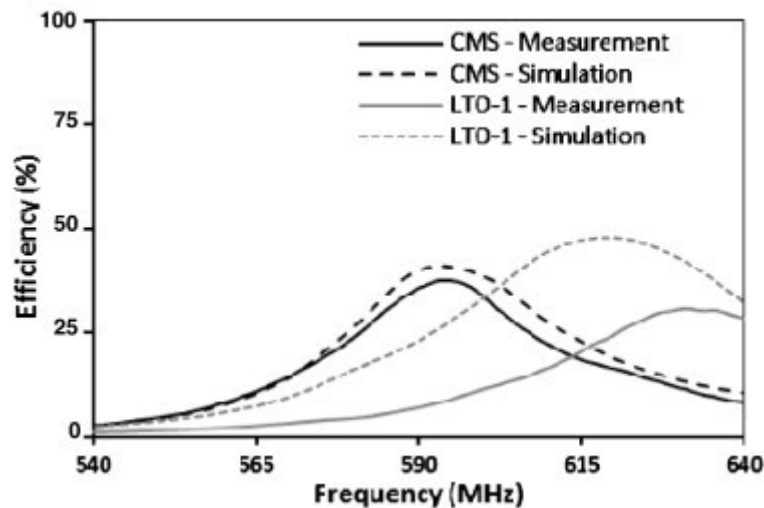


Fig. 6. Efficiency of antennas (measured and simulated) based on LTO-1 dielectric oxide films and low loss commercial CMS capacitor loaded structures.

Comparison of antenna performance based on a LTO capacitor and on a high quality SMD capacitor confirms that the  $\text{La}_2\text{Ti}_2\text{O}_7$  developed material has low losses at working frequencies. Moreover, its moderate dielectric constant has resulted in low capacitances, in the range of few pF, required for a significant miniaturization rate and significant antenna efficiency.

Further technological developments for optimized integration of the capacitor in antenna structure, such as monolithic implementation, can improve the antenna performance. Nevertheless, the miniaturized antenna has almost reached the fundamental limits given by Chu [12], so that a compromise has to be taken between its dimension and efficiency.

## 5. Conclusions

The integration in notch antennas of MIM capacitors based on orthorhombic  $\text{La}_2\text{Ti}_2\text{O}_7$  thin films has been studied numerically and experimentally. The results show important miniaturization rates: 28.5% and 64.2% for two prototypes using 1.5 pF and 3.8 pF MIM capacitors respectively. An adaptation frequency centered at 630 MHz is achieved with the 1.5 pF capacitance, with a total radiated efficiency of 30% for a total volume of  $\lambda_0/9.4 \times \lambda_0/4.3 \times \lambda_0/587$ . These results are close to the fundamental limits underlined in literature and are an illustration of the performance degradation when an antenna is miniaturized.

Despite technological imperfections in the implementation, the performance of the prototype is similar to that of an antenna loaded with a high performance SMD commercial capacitor. Improvements are conceivable by using a monolithic antenna realization, for instance. It could result in a simple and effective application of dielectric thin films in the design of miniature antennas.

## Acknowledgments

The authors gratefully acknowledge the Region Bretagne, CEA-LETI and CNRS for their financial supports.

## References

1. J.L. Volakis, C.-C. Chen, K. Fujimoto. *Small Antennas: Miniaturization Techniques & Applications*. McGraw-Hill, USA (2010)
2. M.C. Scardelletti, G.E. Ponchak, J.L. Jordan, N. Jastram, J.V. Mahaffey. Tunable reduced size planar folded slot antenna utilizing varactor diodes. *IEEE, Proceeding of Radio and Wireless Symposium (RWS), New Orleans, U.S.A. (2010)*, p. 547
3. C.S. Hong. Small annular slot antenna with capacitor loading. *Electron. Lett.*, 36 (2000), p. 110
4. Z. Ma, A.J. Becker, P. Polakos, H. Huggins, J. Pastalan, H. Wu, K. Watts, Y.H. Wong, P. Mankiewich. RF measurement technique for characterizing thin dielectric films. *IEEE Trans. Electron Devices*, 45 (1998), p. 1811
5. B. Ouagague, H.B. El-Shaarawy, S. Pacchini, S. Payan, A. Rousseau, M. Maglione, R. Plana. BST tunability study at DC and microwave frequencies by using IDC and MIM capacitors. *Proceeding of Asia-Pacific Microwave Conference (APMC), Yokohama, Japan (2010)*, p. 1837
6. Y. Lu, A. Ziani, C. Le Paven-Thivet, R. Benzerga, L. Le Gendre, D. Fasquelle, H. Kassem, F. Tessier, V. Vigneras, J.-C. Carru, A. Sharaiha. Perovskite oxynitride  $\text{LaTiO}_x\text{N}_y$  thin films: dielectric characterization in low and high frequencies. *Thin Solid Films*, 520 (2011), p. 778
7. Y. Lu, C. Le Paven-Thivet, R. Benzerga, L. Le Gendre, A. Sharaiha, F. Tessier, F. Cheviré. Influence of the sputtering reactive gas on the oxide and oxynitride  $\text{La-Ti-O-N}$  deposition by RF magnetron sputtering. *Appl. Surf. Sci.*, 264 (2013), p. 533
8. H. Nguyen, R. Benzerga, C. Delaveaud, A. Sharaiha, Y. Lu, C. Le Paven, L. Le Gendre, X. Castel. New thin film varactor for frequency tunable slot antenna. *IEEE, Proceeding of European Conference on Antennas and Propagation (EUCAP), Prague, Czech Republic (2012)*, p. 3595
9. C. Lach, L. Rudant, C. Delaveaud, A. Azoulay. A new miniaturized antenna for ISM 433 MHz frequency band. *Proceeding of European Conference on Antennas and Propagation (EuCAP), Barcelona, Spain (2010)*, p. 1
10. Ansys HFSS (2012)
11. N. Ishizawa, F. Marumo, S. Iwai, M. Kimura, T. Kawamura. Compounds with perovskite-type slabs. *Acta Crystallogr.*, B38 (1982), p. 368
12. L.J. Chu. Physical limitations of omni-directional antennas. *J. Appl. Phys.*, 19 (1948), p. 1163